International Journal of Computer Information Systems and Industrial Management Applications
ISSN 2150-7988 Volume 18(19s) 2026 pp. 913-930
https://doi.org/10.70917/ijcisim-2026-5090
Article

Alkali-Activated Metakaolin as a Low-Carbon Stabilizer for Compressed Earth Blocks: Mechanical, Durability, Thermal and Microstructural Performance

Shaik Kabeer Ahmed [1], Manisha R. Chikane [2], Suguna B Rao 3*, Anuj Kaushikkumar Chandiwala[4], Junead M 5 Shashi Kumar A[6], Ravikiran M [7]

[1]Associate Professor. Department of Civil Engineering, Nitte (Deemed to be University), NMAM Institute of Technology (NMAMIT), Department of Civil Engineering, Nitte, India.
[2]Assistant professor, Department of Chemistry, Jawaharlal Institute of technology,Borawan M.P.
3*Assistant Professor, Department of Civil Engineering, Ramaiah Institute of Technology, Bengaluru 560054
[4]Professor, Department of Civil Engineering, C.K.Pithawala College of Engineering and Technology, Surat- 395009, Gujarat, India
[5]Research Scholar, Department of Civil Engineering, MIT ADT University, Pune
[6]Associate professor, Department of Civil Engineering, SJCIT, Chickballapur, 562101
[7]Research Scholar, Department of Civil Engineering, Ramaiah Institute of Technology, Bengaluru 560054
Email: * suguna_rao@yahoo.com

Abstract: Compressed earth blocks (CEBs) stabilized with ordinary Portland cement (OPC) are extensively used in low-rise construction but exhibit a high embodied carbon footprint. In an effort to minimize the carbon footprint of CEBs, alkali-activated metakaolin (MK) was employed as a low-carbon alternative binder in CEBs prepared from lateritic red soil from Bengaluru, India. Five different systems of CEBs were prepared using 10% OPC as the control and four sodium hydroxide-activated MK systems at 5, 10, 15, and 20% MK to soil ratios. The raw materials were analyzed for particle size distribution, Atterberg limits, XRD analysis, and elemental composition. The Proctor compaction test was performed to determine the optimum moisture content and maximum dry density of each type of CEB. Samples were molded into 70.6 mm cubes and cured in ambient and mild thermal (60 °C) conditions. The samples were tested for compressive strength, dry density, water absorption, fire resistance, and microstructure using scanning electron microscopy (SEM) at 7 days, 28 days of curing, after 24 hours of water exposure, after exposure to 600 °C for 2 hours, and in their raw state. The 10% MK-geopolymer exhibited the highest strength within the geopolymer series (3.83 MPa after full curing, a ≈106% gain over 7-day strength) and retained ≈96% of its ambient strength after being exposed to fire, in comparison to the OPC mixture, which lost 39% of its strength after fire exposure. Furthermore, geopolymer blocks containing 5, 15 and 20% MK experienced disintegration upon immersion in water. SEM analysis of cross sections of geopolymer samples containing 10% MK revealed a more densely-packed and homogeneous structure relative to samples containing higher or lower percentages of MK. Thus, geopolymers containing 10% MK have exhibited various advantageous properties, indicating their potential as an efficient, fire-resilient, and low-carbon cement replacement in the construction of earthen buildings. Furthermore, a compact and exploratory analysis with limited data is also presented in this paper to shed light on the potential use of machine learning in the optimization of these cement-based materials.

Keywords: Compressed earth blocks; Alkali activation; Metakaolin; Geopolymer; Fire resistance; Sustainable construction materials

1. Introduction

Cement and Portland cement are among the materials that underpin the construction of the built environment. Nevertheless, cement production is among the most carbon-intensive construction processes. Cement production releases an estimated 2.4 Gt of CO_2 into the atmosphere each year, accounting for around 6.5-8% of all anthropogenic CO_2 emissions globally [31]. The country with the fifth-highest levels of cement production is India, and the country's cement industry is amongst the largest contributors of carbon dioxide gas from its industrial processes. Furthermore, the production of concrete depletes the available reserves of limestone, clay, and sand resources in the earth, uses large amounts of water in the production process, and creates construction waste. Due to these factors, there is growing interest in alternative construction materials such as earth blocks as a more resource-efficient construction alternative.

Cement blocks are made by compacting moistened soil, with or without a chemical stabilizer, in a manual or hydraulic press. Because unstabilized earth blocks tend to erode and crack when wet, OPC and lime have been traditionally used as soil stabilizers in the formulation of compressed stabilized earth blocks (CSEBs) at rates of 5-10% of the total mass of the block. Though using cement as a stabilizing agent increases the strength of earth blocks when wet, it also introduces carbon emissions into the manufacturing process - an environmental benefit that is intended to be achieved through using earth blocks in the first place. Additionally, the addition of cement to soil can alter the way in which the unstabilized earth naturally, thermally and hygroscopically behaves. Consequently, research into alternatives to OPC as a soil stabilizer has been performed. One of these alternatives is alkali activated binders (AABs) - materials that are formed by reacting aluminosilicate materials (like fly ash, slag, red mud, or metakaolin) with alkaline chemicals (like sodium or potassium hydroxide). Because AABs contain little to no carbon emissions during manufacturing, they are an alternative to OPC in the production of stabilized earth blocks [1,4,12].

Another of the precursors that has been studied for use in producing CEBs is metakaolin (MK), which is produced by calcining clay containing kaolinite at temperatures between 600 and 800 °C [5,6,20,21]. Sore et al. [1] have produced MK geopolymer binders that have shown comparable or superior mechanical performance to the 8% OPC-stabilized CEBs blocks produced from laterite soils from Burkina Faso at binder contents of between 10 and 15%. Furthermore, similar results have been published by Dabakuyo et al. [7] and Kamwa et al. [11,14], who found that the MK-based geopolymer blocks outperformed the cement-stabilized blocks when exposed to fire or heat; MK polymers do not contain the phases that tend to dehydrate within those temperature ranges (above 300-400 °C). Despite these promising results, however, some studies have indicated that MK-based blocks exhibit poor workability, high porosity, and are sensitive to moisture when high dosages of the precursor are used [6,9,10].

Despite the growing literature on lateritic soils and geopolymerization, few studies report data on a single lateritic soil activated with metakaolin across a range of dosages. The geopolymerization behaviour of these systems is known to be soil and source dependent [5,9].

This paper reports on the geopolymerization of a lateritic soil from Bengaluru, India - a soil class often used in construction in South India - using NaOH activated metakaolin at 5, 10, 15 and 20% binder to soil ratios by weight, with comparison to conventional 10% OPC stabilized lateritic soil. The study aims to determine the physical and mineralogical properties of the constituent materials, the mix and compaction requirements for each system, the development of compressive strength, dry density, water absorption and fire resistance with time, the reaction microstructure within the geopolymerized matrix, and to explore whether any models derived from these limited data can be used to guide the development of machine learning models to optimize the preparation of such materials. The results of this study will provide recommendations regarding the stabilization of lateritic soils, as well as provide a basis for future studies on other types of lateritic soils.

Some of the latest developments within the subject of sustainable concrete include the use of supplementary materials, recycled constituents, fibre reinforcements, curing agents, nano-modifications, biological technologies, and digital construction technologies. Authors Dharek et al. [32] investigated the use of concrete that incorporated alumina silicates and determined how these additives influenced the concrete's fresh and hardened concrete properties. Dharek et al. [33] also investigated the effects of incorporating alumina silicates into self-flowing concrete but evaluated the concretes response to exposure to elevated temperatures. Both of these studies indicate the potential use of these types of mineral additives to influence the properties of fresh and hardened concrete.

Digital fabrication has simultaneously emerged as an important direction in sustainable construction. Nair et al. [34] performed a review of the opportunities and challenges of the additive manufacturing of concrete. Similarly, Kolhe et al. [43] developed an affordable three-axis system for the printing of concrete components for the construction of sustainable concrete structures. These investigations suggest that there is a need to optimize the concrete components in relation to the available fabrication technologies.

An alternative strategy for enhancing the cracking resistance of concrete involves the use of fibres and reinforcement components. Authors Sreekeshava et al. [35] investigated the use of polypropylene geo-fabric in concrete and found that it had the potential to modify the performance of the concrete and to control the cracking of the concrete structures containing the additive. Authors Sreekeshava et al. [36] investigated the use of both steel fibres and polypropylene geo-fabric in concrete. The results of this study suggested that the use of these two components in combination had an effect upon the mechanical performance and cracking resistance of the resultant concrete. Authors Bhargavi et al. [42] investigated the use of both steel and polypropylene fibres in geopolymer concrete. The authors reported that the combination of these two types of fibres had an effect upon the mechanical performance of the geopolymer-based concrete. The use of these types of reinforcement components suggests a potential means of enhancing the mechanical performance of both conventional and geopolymer concretes.

Another of the waste materials that has been incorporated into concrete includes industrial and metallic wastes. Venugopal et al. [38] investigated the mechanical characteristics of conventional concrete that utilized steel scrap as one of its components, indicating the feasibility of utilizing steel waste materials. Authors Kumar et al. [40] investigated the inclusion of waste steel scraps into the production of concrete. Each of these studies indicates that it is possible to reduce the demand for conventional resources like steel while also providing an alternative means of utilizing discarded metallic waste materials.

In addition to metallic waste, various by-products from agricultural and industrial processes have also been investigated as potential alternatives to conventional concrete constituents. Authors Natarajan et al. [39] investigated the use of rice husk ash as a potential replacement for some of the fine aggregate that is typically included in conventional concrete. Sunagar et al. [46] investigated the replacement of natural river sand with waste foundry sand, another by-product of an industrial process, and studied the resulting properties of the resultant concrete. Each of these investigations indicates that it is possible to reduce the demand for natural aggregates from fine sources while also utilizing the waste materials from other industrial processes.

Specialized concretes have been developed to meet the specific requirements related to permeability, curing, durability, and consumption of natural resources. Ballari et al. [37] performed experiments to investigate methods of improving the strength of pervious concrete. Reddy et al. [44] investigated the use of polyacrylate-based superabsorbent polymers in recycled aggregate concretes to improve the performance of recycled constituents. Gudadappanavar et al. [47] developed a self-curing concrete that utilized polyethylene glycol and recycled PET to reduce the requirements for curing water and to provide an alternative means of utilizing waste polymeric materials.

The properties of concrete can also be further improved by modifying the matrix of cement within the concrete at the micro- or nanoscale. For instance, Neeraja et al. [41] developed nano-concrete with different proportions of nano-fillers to investigate the reliability of such concretes. These nano-filler particles can alter the properties of the concretes in which they are included, though the extent of their effectiveness is dependent upon the amount of such additive in the cement-based matrix.

Beyond the technologies described in the previous sections of this paper, other biological approaches to enhancing the durability of concrete are also emerging. Authors Gudadappanavar et al. [45] describe an experiment that used microbial remediation techniques to treat cracked concrete samples, leading to an improvement in the durability of the treated concrete. Thus, these authors indicate a shift in the general consideration of concrete from materials that passively degrade over time to materials that can be chemically altered to contribute to the restoration of damaged regions of the concrete.

The technologies that are being discussed in the current literature include aluminosilicate modification [32,33], additive manufacturing [34,43], polypropylene geo-fabric and hybrid fibre reinforcement [35,36,42], pervious concrete [37], recycled metallic waste [38,40], agricultural and industrial by-products [39,46], nano-modification [41], internal curing of recycled aggregate concrete [44], microbial remediation [45], and self-curing systems incorporating recycled polymers [47]. Each of these technologies relate to or relate to the concept of enhancing the sustainability of concrete. However, most of the existing literature on these topics is fragmented and focuses upon each of these different technologies individually. Thus, there is a need for technology that incorporates some of these discussed enhancements in order to provide concrete with improved sustainability, durability, and strength.

2. Materials and Methods

2.1 Constituent materials

Four constituent materials were used in the preparation of the mixtures: a lateritic red soil, metakaolin, Portland cement (of 43 grade, used only in the preparation of the benchmark mixture), and water. The lateritic red soil was excavated from Bengaluru, India (13.0314° N, 77.5658° E). The soil was air-dried and sieved through a 4.75 mm IS sieve to separate the 0/4.75 mm size fraction. The metakaolin was sourced from Gujarat, India. The composition of the metakaolin is represented as calcined kaolinite (at temperatures between 600 and 800 °C for 12 hours). The physical and chemical characteristics of the three constituent materials are detailed in Table 1 and Table 2.

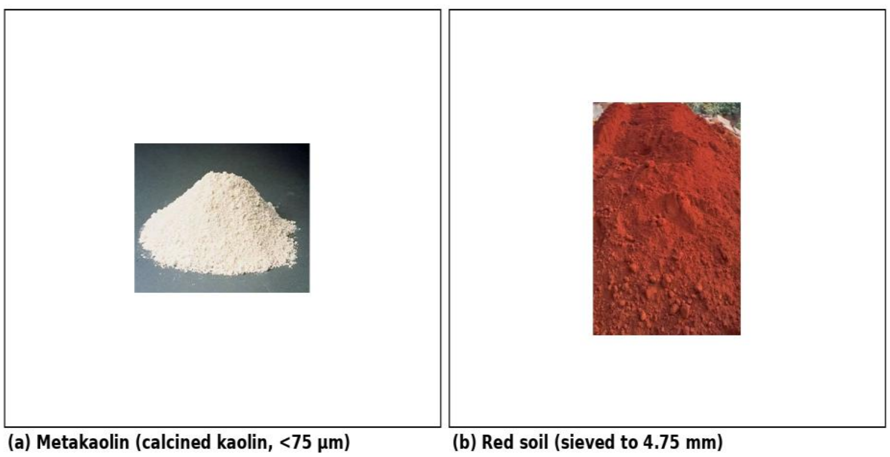

Fig. 1. *Constituent materials: (a) metakaolin; (b) red soil sieved to 4.75 mm.*

Table 1. *Physical and index properties of the constituent materials.*

Property	Red soil	Metakaolin	OPC
Specific gravity	2.54	2.77	3.15
Liquid limit (%)	38.0	–	–
Plastic limit (%)	21.38	–	–
Plasticity index (%)	16.62	–	–
Natural OMC (%) / MDD (g/cm³)	26.5 / 1.721	–	–
pH	7	7	–

Fineness / mean particle size	–	8000–15000 m^2/kg; 1–20 µm	5% retained (90 µm)
Moisture content	–	<3%	–
Standard consistency	–	–	30%
Initial setting time	–	–	30 min
Sand / Silt / Clay (%)	85.4 / 9.8 / 4.8	–	–

Table 2. *Chemical composition of the constituent materials (mass %). Red-soil values are elemental (EDX basis);*

Constituent (element or oxide)	Red soil (elemental)	Metakaolin (oxide)	OPC (oxide)
C / SiO_2	6.7	52–53	22.5
O / Al_2O_3	4.3	36–43	7.5
Na / Fe_2O_3	3.5	1.2–4.2	2.0
Mg / CaO	1.2	0.1–0.5	61.5
Al / MgO	10.0	0.4–0.8	2.0
Si / K_2O	17.5	0.5–1.4	–
K / SO_3	0.8	–	1.0
Ca / $Na_2O{\cdot}K_2O$	4.8	–	1.5
Ti / L.O.I.	0.8	0.4–3.5	–
Fe / –	5.3	–	–

The X-ray diffraction (XRD) patterns of metakaolin and red soil, obtained using Co-Kα radiation at the Ramaiah Institute of Technology, are shown in Fig. 2. The metakaolin pattern displays a broad amorphous "dome" spanning $2\theta \approx 10$–$35°$, indicative of the disordered aluminosilicate structure responsible for its pozzolanic reactivity, with quartz as the only detectable crystalline phase. The red-soil pattern shows sharper crystalline reflections attributable to quartz and goethite superimposed on a comparatively minor amorphous background, consistent with the mineralogy typically reported for lateritic soils [9,18].

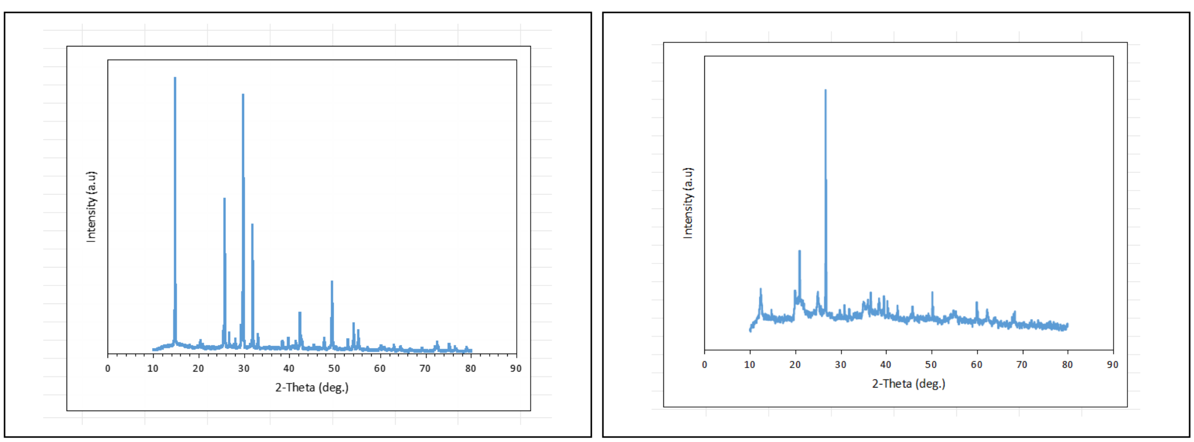

(a) XRD pattern — metakaolin **(b) XRD pattern — red soil**

Fig. 2. *X-ray diffraction patterns: (a) metakaolin; (b) red soil.*

2.2 Mix proportioning

Five stabilization systems were formulated on a dry-mass basis: a benchmark mix with 10% OPC replacement of soil (CEB_{10}%PC), and four geopolymer mixes with 5, 10, 15 and 20% NaOH-activated metakaolin replacement (CEB_{5}%G, CEB_{10}%G, CEB_{15}%G, CEB_{20}%G). For the geopolymer mixes, a 10 M NaOH solution (98%-purity pellets dissolved in distilled water for 24 h) was combined with the dry metakaolin at an alkaline-solution-to-metakaolin mass ratio of 0.8. Design mix proportions are given in Table 3.

Table 3. *Mix proportions of the five stabilization systems (percentage by dry mass of red soil).*

Constituent	CEB_{10}%PC	CEB_{5}%G	CEB_{10}%G	CEB_{15}%G	CEB_{20}%G
Red soil (%)	90	95	90	85	80
Portland cement (%)	10	–	–	–	–
NaOH-activated MK (%)	–	5	10	15	20
Binder / red soil (%)	10	5	10	15	20
Design water / solid (%)	24.12	20.54	14.25	15.25	16.9
Alkaline solution / MK (mass ratio)	–	0.8	0.8	0.8	0.8

Batch quantities for each mould were computed from the bulk density of the compacted dry mix and the internal mould volume, following:

$$\gamma = \frac{W}{V} \tag{1}$$

where γ is bulk density (g/cm³), W is the mass of dry mix (g), and V is the internal mould volume (cm³); the 70.6 mm cube mould (V = 351.9 cm³) was used for mechanical specimens and the standard Proctor mould (V = 989.6 cm³) for compaction testing.

2.3 Specimen preparation, stabilization chemistry and curing

For the geopolymer route, the dry mix (red soil + metakaolin) was homogenized manually for 10 min, after which water and the NaOH activator were added at a combined dosage governed by the optimum moisture content of the corresponding dry mix, W^{G}_{i}, less the alkaline-solution contribution S_a:

$$E_{WG} = \frac{W_{Gi} \times M_d}{100} - S_a \tag{2}$$

where Ew^{G} is the mass of additional water required (g), M^{d} is the mass of the dry mix (g), and the subscript i denotes the metakaolin dosage level (5, 10, 15 or 20%). For the cement route, water was added directly at the optimum moisture content of the red-soil/cement dry mix, W^{c}:

$$E_{WC} = \frac{W_{C} \times M_d}{100} \tag{3}$$

The mixtures were homogenised manually with trowels and compacted by hand with a custom-made compacting tool into two mould sizes: 70.6 × 70.6 × 70.6 mm cubes for mechanical tests and 190 × 90 × 90 mm blocks for dimensional tests. Both types of geopolymers were wrapped in plastic film for curing for 7 days at ambient temperature (30 ± 5 °C) and for an additional 7 days at 60 ± 2 °C in an oven (14 days total). Cement specimens were cured for 21 days at ambient temperature to allow for adequate strength gain from the hydration reaction of OPC particles [2,3,6]. The different steps of the experiments are shown in Fig. 3.

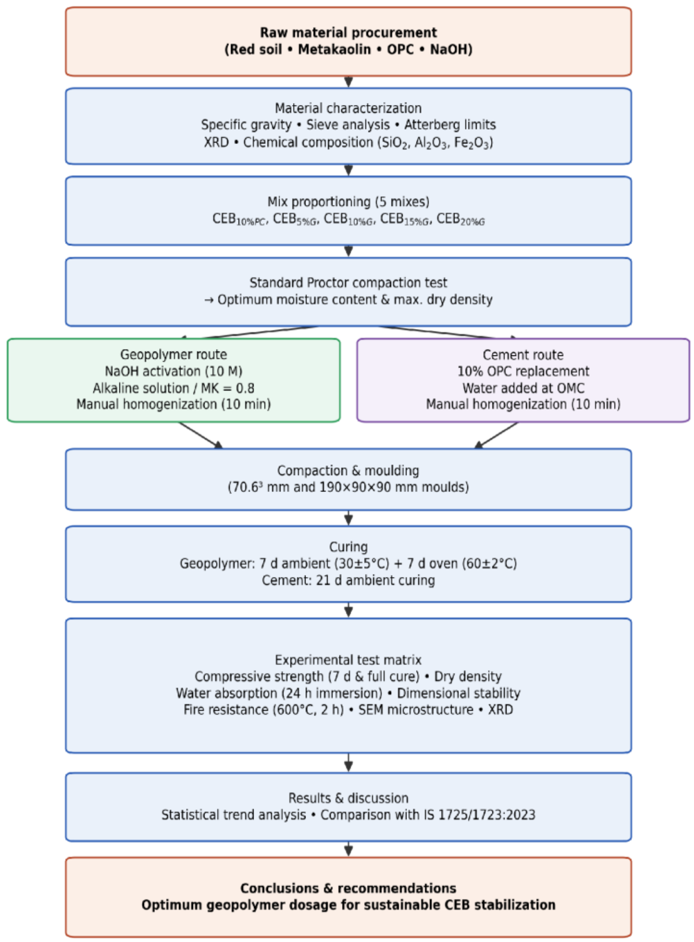

Fig. 3. *Overall experimental methodology adopted in this study.*

2.4 Test methods

Specific gravity of the red soil was determined by the pycnometer method:

$$G_s = \frac{M_2 - M_1}{(M_2 - M_1) - (M_3 - M_4)} \tag{4}$$

where M_1, M_2, M_3 and M_4 are, respectively, the mass of the empty pycnometer, pycnometer with dry soil, pycnometer with soil and water, and pycnometer filled only with water. Particle size distribution was obtained by sieve analysis and Atterberg limits by the Casagrande method (IS 2720 Part 2; IS 9259), with moisture content computed as:

$$w(\%) = \frac{W_2 - W_3}{W_3 - W_1} \times 100 \tag{5}$$

using the mass of the container (W_1), container with wet soil (W_2), and container with oven-dried soil (W_3). The optimum moisture content and maximum dry density are obtained through the standard Proctor test for each dry mix of soil. The dry density is obtained by dividing the bulk density by (1+ w), where w is the moisture content. The compressive strength is determined on 70.6 mm cubes as per IS 3495 (Part 1) at a uniform rate of 7 ± 1 N/mm²/min at 7 days and full curing age. The dry density is calculated from the oven-dried mass of the specimen (110 ± 5 °C to constant mass) and the volume of the full size specimen. The water absorption is determined after soaking the specimen for 24-h in water after oven-drying the specimen to constant mass:

$$W_{abs}(\%) = \frac{M_2 - M_1}{M_1} \times 100 \quad (6)$$

where M_1 and M_2 are the oven-dry mass and the saturated mass after 24 h immersion, respectively (IS 1723:2023 limit: ≤18%). Dimensional stability was checked per IS 5454. Fire resistance was evaluated by exposing specimens to 600 °C for 2 h in a muffle furnace, cooling to room temperature, and re-testing compressive strength; the residual strength index was computed as:

$$RSI(\%) = \frac{f'_{c,fire}}{f'_{c,ambient}} \times 100 \quad (7)$$

Microstructural characterization was performed by scanning electron microscopy (SEM, Zeiss, secondary-electron mode, 3.00 kV) at the Nitte Meenakshi Institute of Technology, Bengaluru. Representative test apparatus is shown in Fig. 4.

Fig. 4. *Test apparatus: (a) compression testing machine; (b) oven used for constant-mass drying; (c) muffle furnace used for the 600 °C fire-resistance test.*

3. Results and Discussion

3.1 Particle size distribution and Atterberg limits

Fig. 5 presents the grading curves of the red soil and metakaolin. The red soil consists of 85.4% sand, 9.8% silt and 4.8% clay particles (by the classification adopted in Table 1), indicating it is well graded between 0.075 and 4.75 mm; the metakaolin is entirely finer than 0.6 mm. The liquid limit of the red soil is 38% and its plasticity index is 16.62%, indicating that it is of low to medium plasticity, which is generally considered to be a suitable plasticity range for construction of stabilized earth buildings [9,18]. Soils of low plasticity are generally preferred for the production of CEBs, since the excessive clay content and plasticity lead to cracking of the resulting CEBs when they dry, and due to the insufficient fines content in soils of low plasticity, the resulting CEBs may not be able to maintain their shape during the demoulding process.

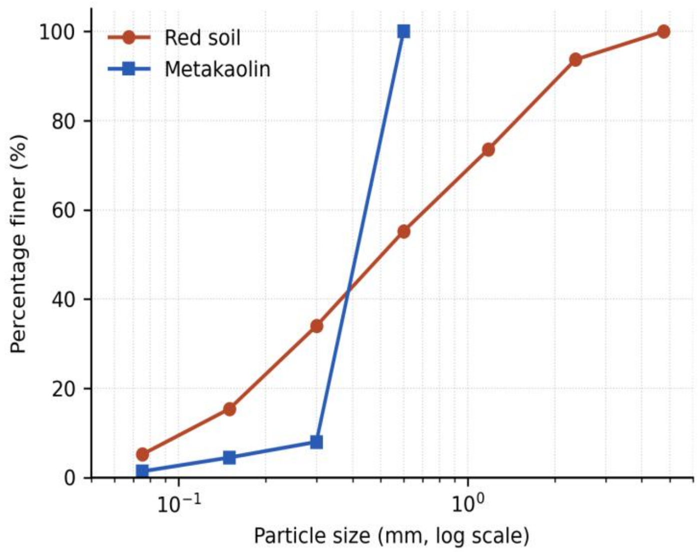

Fig. 5. *Particle size distribution (grading curves) of red soil and metakaolin.*

3.2 Compaction characteristics

Fig. 6 displays the Proctor compaction curves for all five dry mixes. The OMC and MDD for each mix are highlighted on the curves in Table 4. The OPC mix has the highest MDD of 1.71 g/cm³ at the highest content of 22.5% OMC. As the metakaolin content increases in the mixes, the MDD decreases from 1.68 g/cm³ for 5% MK to a minimum of 1.51 g/cm³ at 10% MK. It then increases slightly at 15-20% MK with a minimum OMC of 15.5% occurring at 10-15% MK. The metakaolin particles have a lower density and fineness relative to the red soil particles. Additionally, the MDD of the mixes with NaOH activator indicates that the addition of NaOH alters the amount of water that is required to be present in the mixes to be set to achieve the MDD relative to the mix with granular cement only [18].

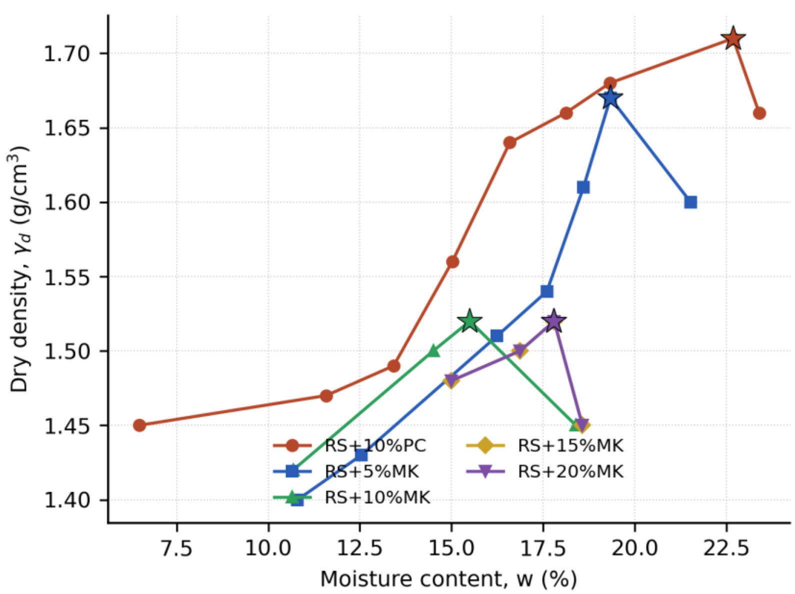

Fig. 6. *Standard Proctor compaction curves for the five stabilization systems (stars denote the optimum moisture content / maximum dry density of each mix).*

Table 4. *Optimum moisture content (OMC) and maximum dry density (MDD) of each mix, from the compaction curves in Fig. 6.*

Mix	CEB_{10}%PC	CEB_5%G	CEB_{10}%G	CEB_{15}%G	CEB_{20}%G
OMC (%)	22.5	19.1	15.5	15.5	17.6
MDD (g/cm³)	1.71	1.68	1.51	1.53	1.52

3.3 Compressive strength development

Fig. 7 presents the compressive strength of the samples at 7 days and at full curing age (14 days for geopolymer mixes and 21 days for the OPC mix). All mixes exhibited a considerable increase in strength between 7 and 21 days of curing as geopolymerization continued for the MK-based mixes during the 60 °C phase of curing and hydration reactions occurred for the OPC mix. The OPC-based mix reached the highest strength values with 5.21 MPa at 21 days. For the geopolymer mixes, the 10% MK-based mix exhibited the highest strength value at 21 days of 3.83 MPa, which is an increase of approximately 106% from its 7-day value of 1.86 MPa. The 15% MK-based mix had a full-curing strength of 3.50 MPa, which meets the minimum strength requirement of 3.5 MPa as specified in IS 1725:2023. However, the 5% and 20% MK-based mixes failed to reach the minimum requirement for geopolymerization-based cement, with strength values of 2.30 MPa and 2.06 MPa at 21 days, respectively. The dosage of MK in each mix and the resulting strength of each mix is discussed in Section 4 of this paper. Results showed that 10% MK dosage exhibited the best reaction between the activator and precursor elements of the geopolymerization reaction. Any dosage beyond this amount led to unreacted MK that acted as an inert filler in the cement mixtures, as proven in Section 3.6 on the insolubility of MK in alkaline solutions.

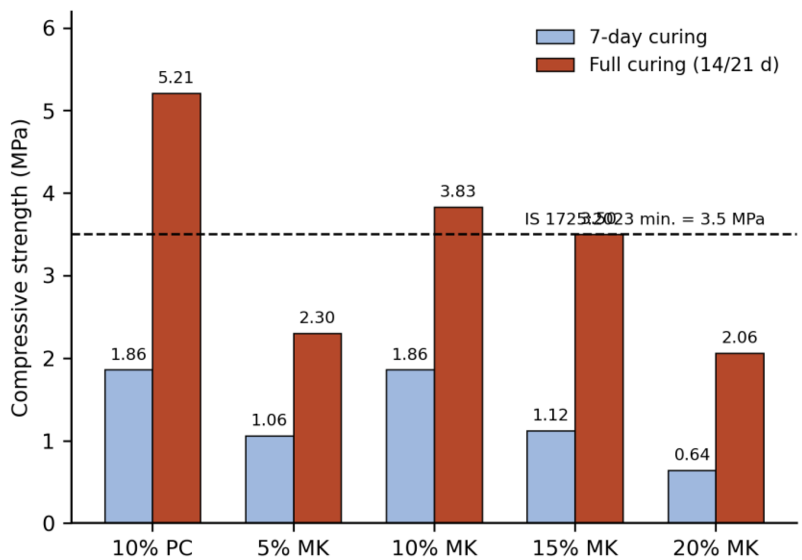

Fig. 7. *Compressive strength at 7-day and full curing age for the five mixes, compared with the IS 1725:2023 minimum requirement (3.5 MPa).*

3.4 Water absorption and dry density

Fig. 8 presents the results of dry density and 24-h water absorption tests. Only the 10% MK and 10% OPC mixes met the minimum dry density of 1750 kg/m³ recommended by the IS (1748 and 2049 kg/m³, respectively). The 5%, 15%, and 20% MK mixes fell short of the recommended dry density (1364-1603 kg/m³). Water absorption could only be measured for the OPC and 10% MK mixes, which measured 14.25% and 17.26%, respectively (within the 18% limit set by the IS). The 5%, 15%, and 20% MK mixes disintegrated during the 24-h water immersion period.

The two mixes that demonstrated the ability to survive immersion (10% OPC and 10% MK) are the same that exhibited the highest dry densities; the insufficient density and reaction of MK at the other percentages resulted in the development of pores within the concrete that allowed for the softening of the concrete during the water immersion period. Thus, each of these independent test methods lead to the same conclusion: the efficiency of the reaction of MK at 10% is the factor that primarily contributes to the strength of the MK concrete.

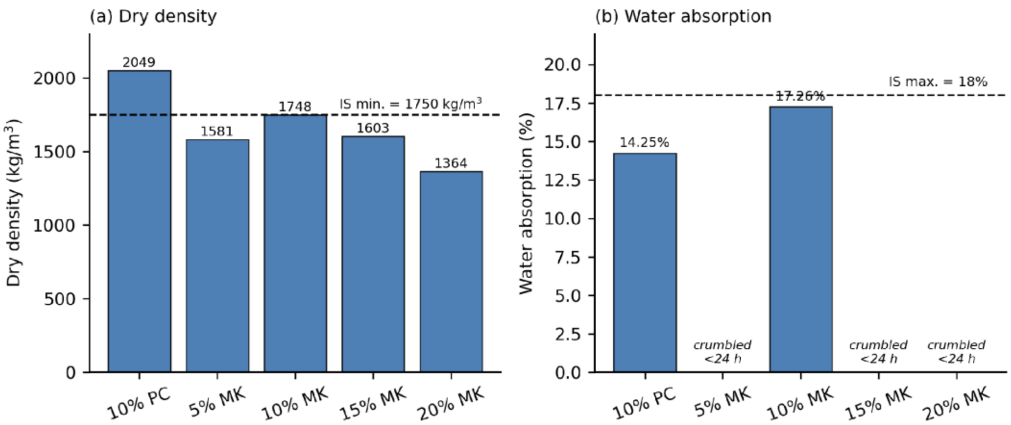

Fig. 8. *(a) Dry density and (b) 24-h water absorption of the five mixes, compared with IS 1725/1723:2023 limits. Mixes marked "crumbled" disintegrated before the 24-h measurement could be taken.*

3.5 Fire and thermal resistance

Fig. 9 illustrates the residual compressive strength of each type of block after exposure to 600 °C for 2 h, compared to their strength at ambient temperatures when fully cured. The OPC-stabilized blocks exhibited a loss of around 39% of their strength at ambient temperatures (from 5.21 to 3.15 MPa). This loss of strength is likely due to the dehydration of the C-S-H and portlandite compounds within the blocks at temperatures above 300-400 °C. In contrast, the 5% and 10% MK geopolymer mixes retained all of their strength (150% and 96% retention, respectively; the apparent gain in strength for the 5% MK blocks is likely due to the completion of the low-temperature geopolymerization reaction during exposure to the furnace [2,3]). The 15% and 20% MK geopolymer mixes, however, only retained 57% and 75% of their strength, respectively, likely as a result of the compounding of the porosity of these mixes (Section 3.6) with cracking due to thermal degradation. Thus, the MK geopolymer mixes that are stabilized with 5-10% MK exhibit an advantage over both OPC and geopolymer mixes that are overdosed with MK; this same finding was reported for other alkali-activated masonry systems [2,3,7].

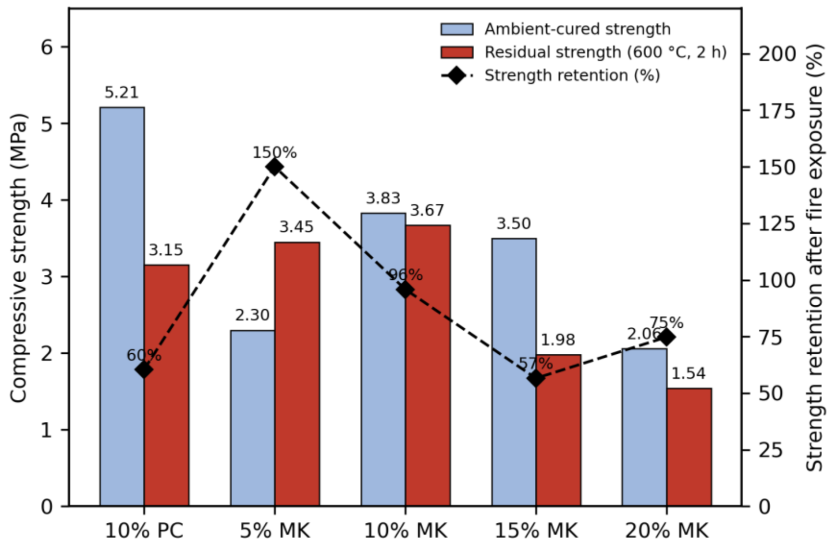

Fig. 9. *Ambient versus residual (post-fire, 600 °C/2 h) compressive strength and strength-retention ratio for the five mixes.*

3.6 Microstructural characterization (SEM)

Representative SEM micrographs (10.00 kX, secondary-electron mode) of each mix are presented in Fig. 10. SEM images of the OPC-stabilized specimen displayed a moderately dense structure consisting of needle-like ettringite crystals incorporated with fibrous C-S-H phases (Fig. 10a). The 5% MK specimen revealed a relatively loose and porous structure with few C-S-H crystals growing between the soil particles (Fig. 10b). The 10% MK specimen displayed the most homogeneous structure within the geopolymer series containing fibrous C-A-S-H/N-A-S-H phases that bonded the soil particles together (Fig. 10c). An increasing number of angular metakaolin agglomerates are visible within the 15% and 20% MK geopolymers that are not reacted with the alkaline solution due to the fixed alkali solution to metakaolin ratio of 0.8 that was used to prepare the geopolymers. An excess of metakaolin can lead to the formation of "lumps," which are the agglomerates of un-reacted metakaolin particles in relation to the amount of available alkaline solution to initiate the geopolymerization reaction [6,9].

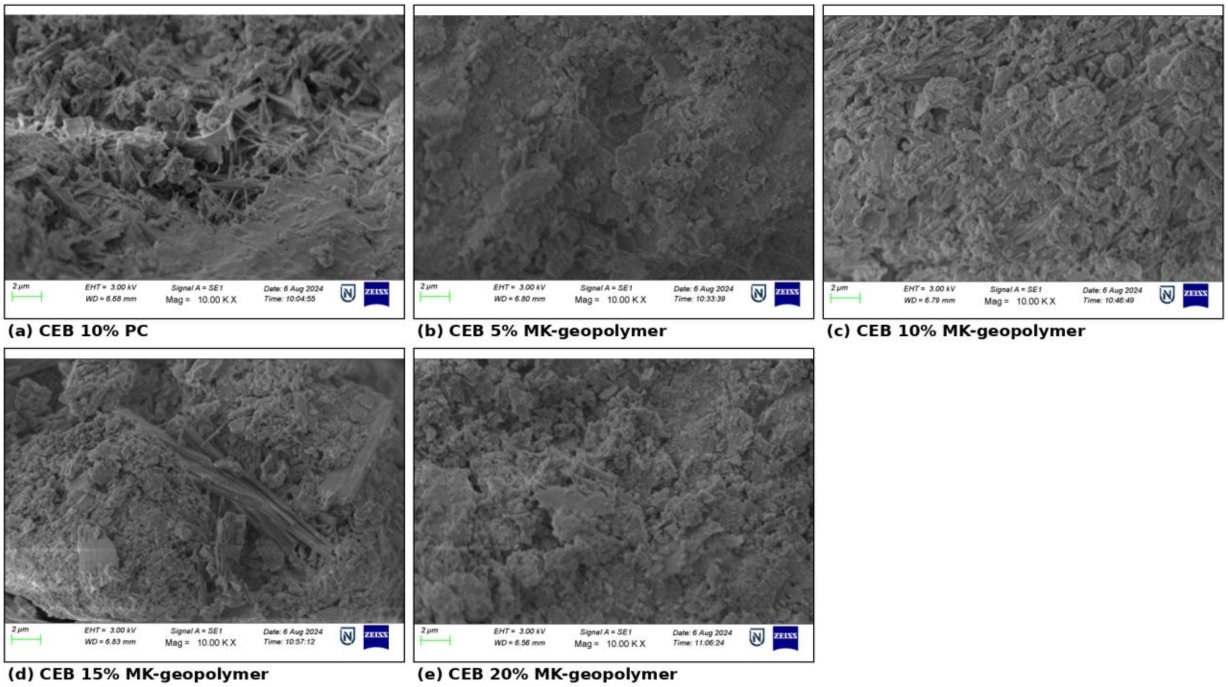

Fig. 10. *Representative SEM micrographs (10.00 kX) of: (a) CEB_{10}%PC; (b) CEB_{5}%G; (c) CEB_{10}%G; (d) CEB_{15}%G; (e) CEB_{20}%G.*

The geopolymerization reaction of metakaolin in alkaline activation media can be represented in simplified schematic form as reaction of the metakaolin with sodium hydroxide and water to form a three-dimensional alkali-aluminosilicate gel [12]:

$Al_2Si_2O_7$ (metakaolin) + NaOH + H_2O → Na^+ + $[Al(OH)_4]^-$ + $[SiO(OH)_3]^-$ (dissolution)

Na^+ + $[Al(OH)_4]^-$ + $[SiO(OH)_3]^-$ → (Na^+)-(-Si-O-Al-O-)$_n$ · wH_2O (N-A-S-H gel, polycondensation)

The SEM observations of the extent of geopolymerization within the samples is strongest at compositions of 10% MK (where the ratio of alkaline solution to metakaolin precursor is believed to most completely match the available reactive surface area of the metakaolin particles) and weakest at compositions of 15-20% MK (where the amount of activator is diluted across a larger mass of precursor material).

3.7 Comparison with published benchmarks

Table 5 presents a comparison between the results of the present study and some of the published data regarding metakaolin-geopolymer-stabilized CEBs. The strengths of 3.5-3.83 MPa that are obtained in the current study for CEBs that are 10-15% MK are within the same range as those of Sore et al. [1], who found that geopolymer content of 15% was comparable to 8% OPC in their treatment of laterite soils from Burkina Faso, though they are somewhat lower than the 4.163 MPa strength of Dabakuyo et al. [7], who used both metakaolin-geopolymer and sugarcane-molasses additives to their soil stabilizers. These differences are due to the differences in the soils that were tested, activator concentration (10 M NaOH versus 12 M [1]), and curing duration, all of which are factors that are recognized to have an influence upon geopolymer-based soil stabilizers in general, as discussed in Section 1.

Table 5. *Comparison of the present results with selected published metakaolin/geopolymer-stabilized CEB studies.*

Study	Precursor / activator	Optimum dosage	Reported strength
Present study	Metakaolin / 10 M NaOH	10% MK	3.83 MPa (14 d)

Sore et al. [1]	Metakaolin / 12 M NaOH	15% geopolymer	≈ comparable to 8% OPC
Dabakuyo et al. [7]	Metakaolin-geopolymer + molasses	10% MKG + 0% SM	4.163 MPa (28 d)
Kamwa et al. [11]	Pozzolana-phosphate geopolymer	study-specific	meets minimum CEB strength

4. Preliminary Data-Driven Trend Analysis

One of the aims of many recent publications in the field of CEB and geopolymer concretes is to develop surrogate models based on machine learning methods - such as artificial neural networks (ANN), random forests (RF), XGBoost gradient boosting models (XGBoost) and support-vector regression (SVR) - to be able to replace the use of empirical models for predicting properties such as strength, density or durability of geopolymer concretes. Furthermore, these surrogate models are often developed using datasets similar to that which was compiled in this study, as summarized in Table 6. For instance, Table 6 includes five mixes of geopolymer concretes (or ten if each mix is represented at both 7 and 28 days), each with several different input variables to the system (such as type of binder, dosage of binder, water to solid ratio and curing age) and several different output variables for the concretes (such as compressive strength, dry density and water absorption).

It is important to state plainly what this dataset can and cannot support. A robust benchmarking of different types of ANN, RF, XGBoost, and SVR models would require the use of a training set large enough to enable the model to learn beyond the specific concretes and CEB mix designs that were used to fit the models; similar ANN-based studies that have aimed to determine the strength of both concrete and CEB have used training sets that contain anywhere from several dozen to several hundred different mixes of concrete or CEB. In this case, however, the training set contains only five different mixes of concrete (or only four different dosage levels of the geopolymer series). Thus, any ANN, RF, XGBOOST, or SVR model that is fitted to these data and that attempts to make predictions would necessarily be interpolating between the available data points; it would not have sufficient data to learn from points beyond those that were used to fit the model. In other words, the modeling of these five mixes with such a model would lead to a misrepresentation of the capabilities of such models. For these reasons, no such model is presented in this study.

Table 6. *Consolidated feature–target dataset compiled from the present experimental programme*

Mix	Binder type	Dosage (%)	Curing age (d)	Strength (MPa)	Dry density (kg/m³)	Water absorption (%)
CEB_{10}%PC	OPC	10	7	1.86	2048.9	14.25
CEB_{10}%PC	OPC	10	21	5.21	2048.9	14.25
CEB_{5}%G	MK-geopolymer	5	7	1.06	1580.9	n/a (crumbled)
CEB_{5}%G	MK-geopolymer	5	14	2.30	1580.9	n/a (crumbled)
CEB_{10}%G	MK-geopolymer	10	7	1.86	1747.7	17.26
CEB_{10}%G	MK-geopolymer	10	14	3.83	1747.7	17.26
CEB_{15}%G	MK-geopolymer	15	7	1.12	1602.7	n/a (crumbled)

CEB_{15}%G	MK-geopolymer	15	14	3.50	1602.7	n/a (crumbled)
CEB_{20}%G	MK-geopolymer	20	7	0.64	1364.0	n/a (crumbled)
CEB_{20}%G	MK-geopolymer	20	14	2.06	1364.0	n/a (crumbled)

Figure 11 depicts the fit of a second-order polynomial equation to the data for each of the four mix designs (R^2 = 0.99). As with the plots of strength vs. MK dosage for each of the four mixes in Fig. 10, the apparent optimum of ≈12% MK is close to the experimental optimum of 10% MK for the mixes determined in Section 3.3. Furthermore, since there are only four data points in the data set, the R^2 value of the fitted polynomial is close to the mathematical expectation that a polynomial fit to a data set of only four points will have such a high value for R^2; thus, these results are typical of fits to such a small data set.

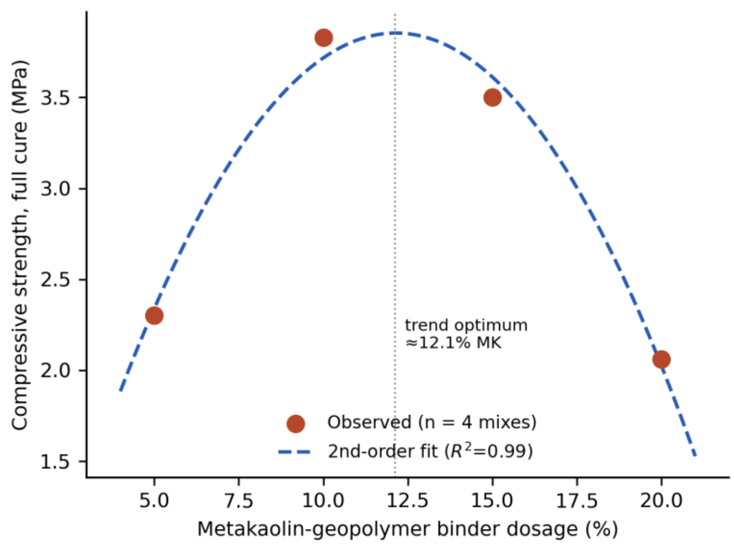

Fig. 11. *Illustrative second-order trend fit of full-cure compressive strength versus metakaolin-geopolymer dosage*

4.1 Recommended framework for a validated ML pipeline

While the framework presented in this paper was based on a relatively narrow range of geopolymer compositions and properties, a move from describing the existing trends in such properties to validating an ML-based tool for predicting those properties can be made through the framework suggested for ANN-based prediction of the compressive strength of cement and geopolymer-based materials in existing literature. Thus, to develop a truly validated ML-based framework for predicting the compressive strength of geopolymer-based materials, specimens can be prepared according to a significantly expanded range of variables (such as dosage, activator concentration, and curing age) and in finer increments (as with 2 to 3% steps in dosage, for example), preparing at least 3 to 5 samples of each type of geopolymer-based material to account for inherent material variability, and creating data sets that contain at least 100 specimens (as is typically used in published studies of such materials); the data can contain the following sets of variables: the type of binder that is used (such as fly ash, slag, or metakaolin), the dosage of that binder, the amount of activator that is used, the water-to-solid ratio, the age of the material after which it is cured, the temperature at which it was cured, and properties of the soil from which the geopolymer was sourced; the target variables for each specimen will be the compressive strength of the resulting material, as will be its dry density and water absorption; standard preprocessing methods can be applied to the data to compensate for any missing data or to normalize the variables; an ANN can be developed that incorporates variables to create a model with 1 or 2 hidden layers and ReLU activation functions, with sizes for the layers that are appropriate to the data set to avoid overparameterizing the model; the developed ANN can be compared to models based on random forests, XGBoost models, and support vector regression models; the developed models can be validated through cross-validation methods (such as k-fold cross-validation or repeated k-fold cross-validation), as well as through a test data set that was not used during training; the models can be reported through measures of the coefficient of determination (R^2), root mean square error (RMSE), mean absolute error (MAE), and mean absolute percentage error (MAPE), each with confidence intervals; and methods of feature importance, such as SHAP analyses can be performed to determine which variables are most important to the prediction of compressive strength, and that result can be compared to the results from SEM analyses to determine which variables should have the most influence on the compressive strength of the samples of geopolymer-based materials (and their correlation with the influence of those variables on that strength). This roadmap, together with the dataset presented in Table 6, serves as a starting point for future work in this area.

5. Conclusions

Of the five systems of stabilisation tested, 10% NaOH-activated metakaolin (alkaline solution/MK mass ratio of 0.8) provided the best overall balance of strength (3.83 MPa at full cure - exceeding the minimum of 3.5 MPa as per IS 1725:2023), dry density (1748 kg/m³ - meeting the threshold of 1750 kg/m³), and fire resistance (retained 96% of its strength after exposure to 600 °C for 2 hours).

The 15% MK system met the minimum requirement for strength (3.50 MPa) but did not fare as well in fire resistance (only 57% of its strength was retained after the same fire exposure). Furthermore, as the specimens disintegrated upon immersion in water, it was not possible to determine the rate of water absorption of this system.

• The 5% and 20% MK dosages were, respectively, insufficiently and excessively reactive relative to the activator ratio used, resulting in geopolymer blocks that failed the water absorption durability screen - a property that must be optimized in MK geopolymer systems.

• Cement stabilization at 10% OPC produced the highest ambient strength value of 5.21 MPa but experienced a 39% loss of strength after exposure to fire relative to MK and MK+10% MK block strength increases, indicating a trade-off between sustainability and fire resistance that favours MK geopolymer stabilization at moderate MK dosages.

• SEM analysis of blocks revealed a dense and homogeneous reaction product structure at 10% MK dosage relative to samples at 5%, 15%, and 20% MK, which provides a possible explanation for the differing strength values of the samples of different MK dosages.

A preliminary exploratory regression of the five-mix dataset reveals the presence of an optimum strength dosage range of approximately 10-12%. While the machine learning models have been statistically validated using much smaller datasets, obtaining a sufficiently large and representatively varied dataset of mix samples is required to train the models for mix optimization. Such a framework and dataset is provided in Section 4 of this report.

5.1 Limitations and future scope

The study was performed using a single soil source and only a single specimen of each soil mixture. Thus, statistical analyses could not be performed on the specimens to determine, for instance, the standard deviation of strength of each mixture. Additionally, while the solid-to-water ratios included in the preparation of the specimens are published in Table 3, the actual amounts of water added to each batch to achieve such a ratio are published in Table 4; the two tables publish slightly different ratios, but both are published for transparency of the testing. Each of the specimens were tested at a single fire temperature (600 °C) and duration of fire exposure (2 hours). Future testing could expand to various fire temperatures, fire rates of heating, and the analysis of the resulting specimens for remaining structural elements. Finally, while the datasets published in this report provide a starting point for analysis of the effect of various dosages, activators, soils, and curing conditions, future testing should expand into these additional variables to provide a more thorough understanding of aspects of soil cement.

REFERENCES

1. S. O. Sore, A. Messan, E. Prud'Homme, G. Escadeillas, and F. Tsobnang, “Stabilization of compressed earth blocks (CEBs) by geopolymer binder based on local materials from Burkina Faso,” *Constr. Build. Mater.*, vol. 165, pp. 333–345, 2018.
2. C. Ferone, F. Colangelo, R. Cioffi, F. Montagnaro, and L. Santoro, “Mechanical performances of weathered coal fly ash based geopolymer bricks,” *Procedia Eng.*, vol. 21, pp. 745–752, 2011.
3. J. Cai, X. Li, J. Tan, and B. Vandevyvere, “Thermal and compressive behaviors of fly ash and metakaolin-based geopolymer,” *J. Build. Eng.*, vol. 30, p. 101307, 2020.
4. P. O. Awoyera, A. Adesina, A. Sivakrishna, R. Gobinath, K. R. Kumar, and A. Srinivas, “Alkali activated binders: Challenges and opportunities,” *Mater. Today Proc.*, vol. 27, pp. 40–43, 2020.
5. M. Valášková, Z. Klika, J. Vlček, L. Matějová, M. Topinková, H. Pálková, and J. Madejová, “Alkali-activated metakaolins: mineral chemistry and quantitative mineral composition,” *Minerals*, vol. 12, no. 11, p. 1342, 2022.
6. L. Chen, Z. Wang, Y. Wang, and J. Feng, “Preparation and properties of alkali activated metakaolin-based geopolymer,” *Materials*, vol. 9, no. 9, p. 767, 2016.
7. I. Dabakuyo, R. N. Mutuku, and R. O. Onchiri, “Mechanical properties of compressed earth block stabilized with sugarcane molasses and metakaolin-based geopolymer,” *Civ. Eng. J.*, vol. 8, no. 4, pp. 780–795, 2022.
8. K. Mak, C. MacDougall, and A. Fam, “Freeze-thaw performance of on-site manufactured compressed earth blocks: effect of water repellent and other additives,” *J. Mater. Civ. Eng.*, vol. 28, no. 7, p. 04016034, 2016.
9. P. Nshimiyimana, N. Fagel, A. Messan, D. O. Wetshondo, and L. Courard, “Physico-chemical and mineralogical characterization of clay materials suitable for production of stabilized compressed earth blocks,” *Constr. Build. Mater.*, vol. 241, p. 118097, 2020.
10. D. Maskell, A. Heath, and P. Walker, “Use of metakaolin with stabilised extruded earth masonry units,” *Constr. Build. Mater.*, vol. 78, pp. 172–180, 2015.
11. R. A. T. Kamwa, S. Tome, J. Chongouang, I. Eguekeng, A. Spieß, M. N. Fetzer, et al., “Stabilization of compressed earth blocks (CEB) by pozzolana based phosphate geopolymer binder: Physico-mechanical and microstructural investigations,” *Clean. Mater.*, vol. 4, p. 100062, 2022.
12. J. Davidovits, “Geopolymers: Ceramic-like inorganic polymers,” *J. Ceram. Sci. Technol.*, vol. 8, no. 3, pp. 335–350, 2017.
13. P. Ghadir and N. Ranjbar, “Clayey soil stabilization using geopolymer and Portland cement,” *Constr. Build. Mater.*, vol. 188, pp. 361–371, 2018.
14. R. A. T. Kamwa, L. T. Noumbissie, S. Tome, E. Idriss, J. G. D. Nemaleu, B. Tommes, and M. A. Etoh, “A comparative study of compressed lateritic earth bricks stabilized with natural pozzolan-based geopolymer binders synthesized in acidic and alkaline conditions,” *Constr. Build. Mater.*, vol. 400, p. 132652, 2023.
15. H. N. Abhilash, P. Walker, B. V. Venkatarama Reddy, A. Heath, and D. Maskell, “Compressive strength of novel alkali-activated stabilized earth materials incorporating solid wastes,” *J. Mater. Civ. Eng.*, vol. 32, no. 6, p. 04020118, 2020.
16. K. Elert, E. S. Pardo, and C. Rodriguez-Navarro, “Alkaline activation as an alternative method for the consolidation of earthen architecture,” *J. Cult. Herit.*, vol. 16, no. 4, pp. 461–469, 2015.
17. J. F. Muñoz, T. Easton, and J. Dahmen, “Using alkali-activated natural aluminosilicate minerals to produce compressed masonry construction materials,” *Constr. Build. Mater.*, vol. 95, pp. 86–95, 2015.
18. B. V. Venkatarama Reddy and M. S. Latha, “Influence of soil grading on the characteristics of cement stabilised soil compacts,” *Mater. Struct.*, vol. 47, pp. 1633–1645, 2014.
19. S. Cabrera, K. Elert, A. Guilarducci, and A. Margasin, “The effect of local pozzolans and lime additions on the mineralogical, physical and mechanical properties of compressed earth blocks in Argentina,” *Rev. Constr.*, vol. 21, no. 2, pp. 248–263, 2022.
20. P. Koutnik, A. Soukup, P. Bezucha, J. Šafář, and J. Kohout, “Low viscosity metakaolinite based geopolymer binders,” *Constr. Build. Mater.*, vol. 230, p. 116978, 2020.
21. B. Kim and S. Lee, “Review on characteristics of metakaolin-based geopolymer and fast setting,” *J. Korean Ceram. Soc.*, vol. 57, pp. 368–377, 2020.
22. R. Abid, N. Kamoun, F. Jamoussi, and H. El Feki, “Fabrication and properties of compressed earth brick from local Tunisian raw materials,” *Bol. Soc. Esp. Ceram. Vidr.*, vol. 61, no. 5, pp. 397–407, 2022.
23. S. Mkaouar, W. Maherzi, P. Pizette, H. Zaitan, and M. Benzina, “A comparative study of natural Tunisian clay types in the formulation of compacted earth blocks,” *J. Afr. Earth Sci.*, vol. 160, p. 103620, 2019.
24. M. Statkauskas, D. Vaičiukynienė, and A. Grinys, “Mechanical properties of low calcium alkali activated binder system under ambient curing conditions,” *Sci. Rep.*, vol. 14, no. 1, p. 13060, 2024.
25. K. C. Onyelowe, A. Naghizadeh, F. I. Aneke, D. P. Kontoni, M. E. Onyia, M. Welman-Purchase, et al., “Characterization of net-zero pozzolanic potential of thermally-derived metakaolin samples for sustainable carbon neutrality construction,” *Sci. Rep.*, vol. 13, no. 1, p. 18901, 2023.
26. S. Wang, J. Su, Z. Wu, W. Ma, Y. Li, and H. Hui, “Silty clay stabilization using metakaolin-based geopolymer binder,” *Front. Phys.*, vol. 9, p. 769786, 2021.
27. Z. Li, S. Zhang, Y. Zuo, W. Chen, and G. Ye, “Chemical deformation of metakaolin based geopolymer,” *Cem. Concr. Res.*, vol. 120, pp. 108–118, 2019.
28. M. S. Amalkar, M. Ali, and K. S. Jagadish, “Strength of stabilized mud block masonry,” *J. Build. Pathol. Rehabil.*, vol. 6, no. 1, p. 8, 2021.

29. L. Santos de Oliveira, N. P. Barbosa, F. S. Santos, and C. M. de Carvalho, "Stabilization of raw earth through alkaline activation," *Key Eng. Mater.*, vol. 600, pp. 215–224, 2014.
30. C. E. Embom, J. F. N. Bayamack, A. N. O. Ze, J. R. Mache, J. A. Mbey, and V. L. Onana, "Compressed earthen blocks using alluvial clays from Mbam: performance comparison using statistical analysis of cement vs heat-stabilized blocks," *Clay Miner.*, pp. 1–13, 2024.
31. International Energy Agency (IEA), "Cement," IEA, Paris, 2024. Available: iea.org/energy-system/industry/cement.
32. M. S. Dharek, P. Sunagar, K. V. Bhanu Tej, and S. U. Naveen, "Fresh and hardened properties of self-consolidating concrete incorporating alumina silicates," in *Sustainable Construction and Building Materials: Select Proceedings of ICSCBM 2018*, pp. 697–706, Springer Singapore, 2018. doi: 10.1007/978-981-13-3317-0_60.
33. M. S. Dharek, P. Sunagar, K. Harish, K. S. Sreekeshava, S. U. Naveen, and Bhanutej, "Performance of self-flowing concrete incorporated with alumina silicates subjected to elevated temperature," in *Advances in Structural Engineering: Select Proceedings of FACE 2019*, vol. 74, pp. 111–120, Springer Singapore, 2020. doi: 10.1007/978-981-15-5644-9_9.
34. A. Nair, S. D. Aditya, R. N. Adarsh, M. Nandan, M. S. Dharek, B. M. Sreedhara, P. C. Sunagar, and K. S. Sreekeshava, "Additive manufacturing of concrete: Challenges and opportunities," *IOP Conf. Ser. Mater. Sci. Eng.*, vol. 814, no. 1, p. 012022, 2020. doi: 10.1088/1757-899X/814/1/012022.
35. K. S. Sreekeshava, A. S. Arunkumar, M. S. Dharek, and P. Sunagar, "Studies on inclusion of polypropylene (PP) geo-fabric in concrete," in *National Conference on Structural Engineering and Construction Management*, pp. 11–21, Springer International Publishing, 2020. doi: 10.1007/978-3-030-64522-2_2.
36. K. S. Sreekeshava, A. S. Arunkumar, C. R. Ganesh, M. S. Dharek, and P. Sunagar, "Influence of steel fiber with polypropylene (PP) geo-fabric on the performance of concrete," in *Emerging Technologies for Sustainability*, pp. 33–40, CRC Press, 2020. doi: 10.1201/9781003038122-7.
37. S. O. Ballari, S. Pradhan, H. K. Behera, and P. Sunagar, "Experimental study for improving the strength for pervious concrete," *NeuroQuantology*, vol. 20, no. 12, pp. 1353–1359, 2022. doi: 10.14704/nq.2022.20.12.NQ88138.
38. N. Venugopal, L. Emmanual, P. Sunagar, L. Parida, M. Sivaranjani, and M. Santhanakrishnan, "Enhancing the mechanical characteristics of the traditional concrete with the steel scrap," *J. Phys.: Conf. Ser.*, vol. 2272, no. 1, p. 012031, 2022. doi: 10.1088/1742-6596/2272/1/012031.
39. S. Natarajan, S. H. Jeelani, P. Sunagar, S. Magade, S. S. Salvi, and S. Bhattacharya, "Investigating conventional concrete using rice husk ash (RHA) as a substitute for finer aggregate," *J. Phys.: Conf. Ser.*, vol. 2272, no. 1, p. 012030, 2022. doi: 10.1088/1742-6596/2272/1/012030.
40. D. P. Kumar, G. J. N. Gladson, A. Chandramauli, B. Uma, P. Sunagar, and S. H. Jeelani, "Influence of reinforcing waste steel scraps on the strength of concrete," *Mater. Today Proc.*, vol. 69, pp. 1134–1137, 2022. doi: 10.1016/j.matpr.2022.08.122.
41. V. S. Neeraja, V. Mishra, C. P. Ganapathy, P. Sunagar, D. P. Kumar, and L. Parida, "Investigating the reliability of nano-concrete at different content of a nano-filler," *Mater. Today Proc.*, vol. 69, pp. 1159–1163, 2022. doi: 10.1016/j.matpr.2022.08.128.
42. C. Bhargavi, K. S. Sreekeshava, P. Sunagar, M. S. Dharek, and C. R. Ganesh, "Mechanical properties of steel and polypropylene fiber reinforced geopolymer concrete," *J. Mines, Metals & Fuels*, vol. 71, no. 7, 2023. doi: 10.18311/jmmf/2023/35724.
43. A. R. Kolhe, P. Gorde, S. E. Chandgude, J. Khachane, and Sunagar, P., "Design and development of 3 axis 3D printing of sustainable concrete structures and characterization of affordable housing solution," *Rock Soil Mech.*, vol. 44, no. 6, pp. 499–511, 2023. doi: 10.16285/j.rsm.2022.7154.
44. C. R. G. Reddy, B. R. Vinod, S. Wali, and P. Sunagar, "Performance of polyacrylate-based super absorbent polymers in recycle aggregate concrete," *Educational Administration: Theory and Practice*, vol. 30, no. 4, pp. 9836–9841, 2024. doi: 10.53555/kuey.v30i4.5918.
45. B. Gudadappanavar, V. Vijapur, P. Bhagyashri, Raja Gopa Reddy, and P. Sunagar, "Performance analysis of microbial remediated concrete: An experimental evaluation," *Acta Scientiae*, vol. 7, no. 1, pp. 727–738, 2024. doi: 10.54855/actasci.24771.
46. P. Sunagar, L. Hegde, G. Satish Kumar, H. Hema, B. Simpi, and K. Raghu, "Exploring the geological impact on physical, mechanical and chemical properties of concrete with partial replacement of natural river sand by waste foundry sand," *Nanotechnology Perceptions*, vol. 20, no. 8, pp. 1232–1244, 2024. doi: 10.62441/nano-ntp.v20iS8.1465.
47. B. Gudadappanavar, V. A. Hosur, G. B. Deepak, and P. Sunagar, "Advanced self-curing concrete through polyethylene glycol and recycled PET integration: Towards greener construction practices," *International Journal of Environmental Sciences*, vol. 11, no. 16, pp. 1952–1964, 2025. doi: 10.56293/IJES.2025.11.16.222.